0026-895X/08/7303-660–668$20.00
MOLECULAR PHARMACOLOGY
Copyright © 2008 The American Society for Pharmacology and Experimental Therapeutics
Mol Pharmacol 73:660–668, 2008

Vol. 73, No. 3
41038/3303415
Printed in U.S.A.

Identification and Characterization of Two Amino Acids Critical for the Substrate Inhibition of Human Dehydroepiandrosterone Sulfotransferase (SULT2A1)

Lu-Yi Lu, Yin-Cheng Hsieh, Ming-Yih Liu, Yih-Hung Lin, Chun-Jung Chen, and Yuh-Shyong Yang

Department of Biological Science and Technology, National Chiao Tung University, Hsinchu, Taiwan, Republic of China (L.-Y.L., Y.-S.Y.); Life Science Group, Research Division, National Synchrotron Radiation Research Center, Hsinchu, Taiwan (M.-Y.L., Y.-H.L., C.-J.C.); Institute of Bioinformatics and Structural Biology (Y.-C.H.), Department of Physics (C.-J.C.), National Tsing-Hua University, Hsinchu, Taiwan; and National Nano Device Laboratories and Instrument Technology Research Center, NARL, Hsinchu, Taiwan (Y.-S.Y.)

Received August 17, 2007; accepted November 26, 2007

ABSTRACT

Substrate inhibition is a characteristic feature of many cytosolic sulfotransferases. The differences between the complex structures of SULT2A1/DHEA and SULT2A1/PAP or SULT2A1/ADT (Protein Data Bank codes are 1J99, 1EFH, and 1OV4, respectively) have enabled us to elucidate the specific amino acids responsible for substrate inhibition. Based on the structural analyses, substitution of the smaller residue alanine for Tyr-238 (Y238A) significantly increases the K_i value for dehydroepiandrosterone (DHEA) and totally eliminates substrate inhibition for androsterone (ADT). In addition, Met-137 was proposed to regulate the binding orientations of DHEA and ADT in SULT2A1. Complete elimination or regeneration of substrate inhibition for SULT2A1 with DHEA or ADT as substrate, respectively, was demonstrated with the mutations of Met-137 on Y238A mutant. Analysis of the Met-137 mutants and Met-137/Tyr-238 double mutants uncovered the relationship between substrate binding orientations and inhibition in SULT2A1. Our data indicate that, in the substrate inhibition mode, Tyr-238 regulates the release of bound substrate, and Met-137 controls substrate binding orientation of DHEA and ADT in SULT2A1. The proposed substrate inhibition mechanism is further confirmed by the crystal structures of SULT2A1 mutants at Met-137. We propose that both substrate binding orientations exhibited substrate inhibition. In addition, a corresponding residue in other cytosolic sulfotransferases was shown to have a function similar to that of Tyr-238 in SULT2A1.

Sulfation is a widespread biological reaction catalyzed by members of the sulfotransferase (SULT) supergene family. These enzymes catalyze the transfer of a sulfuryl group from 3′-phosphoadenosine 5′-phosphosulfate (PAPS), the universal sulfuryl group donor molecule, to a substrate acceptor group. Cytosolic sulfotransferases catalyze sulfation of small molecules such as drugs, steroid hormones, chemical carcinogens, bile acids, and neurotransmitters (Mulder and Jakoby, 1990; Falany and Roth, 1993; Weinshilboum and Otterness, 1994; Glatt, 1997). Human SULT2A1 [dehydroepiandrosterone (DHEA) sulfotransferase] catalyzes the sulfation of various steroids and their derivatives, including hydroxysteroids such as DHEA, androsterone (ADT), testosterone, estradiol, and many other endogenous steroids (Chen et al., 1996; Falany, 1997; Kakuta et al., 1998). Steroid sulfation has been recognized as an important process for maintaining steroid hormone levels during their metabolism. In humans, dehydroepiandrosterone sulfate is the most prevalent steroid precursor and is one of the major secretory products of both adult and fetal adrenals (Chang et al., 2004).

Substrate inhibition is a common characteristic of sulfotransferases (Marcus et al., 1980; Sugiyama et al., 1984; Ganguly et al., 1995; Raftogianis et al., 1999). The catalysis and inhibition of DHEA and ADT by SULT2A1 have been reported to regulate the homeostasis and metabolism of these compounds and to maintain steroid levels (Chang et al., 2004). Previous studies have suggested that the onset of substrate inhibition is the formation of ternary dead-end complex (Duffel and Jakoby, 1981; Zhang et al., 1998). Furthermore, other kinetic studies also indicate that the dead-

This research was supported by National Science Council, Taiwan, under project NSC 95-2120-M-009-003 and 95-2627-B009-004.
Article, publication date, and citation information can be found at http://molpharm.aspetjournals.org.
doi:10.1124/mol.107.041038.

ABBREVIATIONS: SULT, sulfotransferase; PAPS, 3′-phosphoadenosine 5′-phosphosulfate; PAP, 3′-phosphoadenosine 5′-phosphate; DHEA, dehydroepiandrosterone; ADT, androsterone; MUS, 4-methylumbelliferyl sulfate; *p*NP, *p*-nitrophenol.

end complexes of E/PAP-SO_3/RO-SO_3 and E/PAP/ROH can be formed through either sequential random or ordered Bi Bi kinetic mechanisms (Varin and Ibrahim, 1992; Zhang et al., 1998; Marshall et al., 2000). This indicates that the changes of PAP affinity to sulfotransferase, for example in the different redox states for rat SULT1A1 (Marshall et al., 1997, 2000), can affect substrate inhibition and enzyme activity. Furthermore, the substrate inhibition in SULT1A1 has been studied from X-ray crystal structure and compared with that of SULT1A3, which shares 93% amino acid sequence identity. The presence of two *p*-nitrophenol (*p*NP) molecules in the crystal structure of SULT1A1 explains the cooperativity and inhibition at low and high substrate concentrations, respectively (Gamage et al., 2003; Barnett et al., 2004). The stoichiometry of estradiol binding with human SULT1E1 was shown to have two ligands with one enzyme homodimer. Two binding sites were proposed as the catalytic and allosteric sites, respectively (Zhang et al., 1998). In a separate study, the crystal structure of SULT2A1 shows the presence of two orientations of DHEA in SULT2A1 (Rehse et al., 2002). There are interesting similarity and difference between SULT1A1 and SULT2A1 regarding their substrate binding orientations. However, the substrate inhibition in SULT2A1 has not been studied in detail.

Structural alignments among the complex structures of SULT2A1/ADT, SULT2A1/DHEA, and SULT2A1/PAP (Pedersen et al., 2000; Rehse et al., 2002; Chang et al., 2004) reveal spatial variation of amino acids in different substrate and PAP binding states. We herein describe experimental considerations that lead us to propose that two of the amino acids, Tyr-238 and Met-137, are residues responsible in regulating substrate inhibition. Finally, we give another experimental example to demonstrate that the corresponding Tyr-238 residues of other cytosolic sulfotransferases possess a function similar to that of SULT2A1.

Materials and Methods

Materials

Pfu Turbo DNA polymerase was purchased from Stratagene (La Jolla, CA), and MUS, 4-methylumbelliferone, DHEA, ADT, PAP, PAPS, *p*-nitrophenol, dopamine, glutathione (reduced form), and dithiothreitol were purchased from Sigma (St. Louis, MO). Potassium phosphate (dibasic) was obtained from Mallinckrodt Baker (Phillipsburg NJ). DEAE Sepharose fast flow, glutathione transferase Sepharose fast flow, and Sephacryl *S*-100 HR were obtained from GE Healthcare (Chalfont St. Giles, Buckinghamshire, UK). All other chemicals were obtained commercially at the highest purity possible.

Methods

Site-Directed Mutagenesis of the cDNA Encoding SULT2A1, SULT1A1, and SULT1A3. Site-directed mutagenesis was performed with *PfuTurbo* DNA polymerase using QuikChange (Stratagene, La Jolla, CA). All primers for mutagenesis were purchased from Mission Biotech Co., Ltd. (Taiwan). Wild-type SULT2A1, SULT1A1, and SULT1A3 cDNA incorporated in the pGEX-2TK expression vector were used as templates in conjunction with specific mutagenic primers. Mutated cDNA sequences were confirmed using an ABI Prism 377 DNA sequencer (Applied Biosystems, Foster City, CA) following the standard protocol.

Expression, Purification, and Characterization of Wild-Type and Mutants of SULT2A1, SULT1A1, and SULT1A3. The expression and purification of SULT2A1, SULT1A1, and SULT1A3 were described previously (Sakakibara et al., 1998). Molecular weight of wild-type (homodimer) and V260E mutant (monomer) of SULT2A1 was estimated by gel filtration chromatography. A homogeneous protein was obtained as determined by SDS-polyacrylamide gel electrophoresis (Laemmli, 1970).

Enzyme Assay. The activities of wild-type and mutant SULT2A1 were determined according to the change of fluorescence based on a coupled-enzyme assay method (Chen et al., 2005). The fluorescence of 4-methylumbelliferone at 460 nm was measured upon excitation at 355 nm. The reaction mixture with a final volume of 1 ml consisted of 100 mM potassium phosphate buffer at pH 7.0, 5 mM 2-mercaptoethanol, 20 μM PAPS, 2 mM MUS, 5.4 μg of K65ER68G (Yang et al., 1996) of rat SULT1A1, SULT2A1, and 5 μM of DHEA or ADT at 37°C. A linear response was obtained when 1.49 to 14.9 nM (0.1–1 μg) SULT2A1 was added in the standard assay condition. In the reaction condition, excess amount of K65ER68G of rat SULT1A1 was added to catalyze the regeneration of PAPS so that the production of PAP catalyzed by SULT2A1 could not accumulate (Chen et al., 2005). The reaction condition for SULT1A3 standard assay was similar to that for SULT2A1 assay except that the reaction mixture contained 1.5 to 7.3 nM (0.1 to 0.5 μg) SULT1A3 and 30 μM dopamine at 37°C to replace SULT2A1 and DHEA or ADT, respectively. The control experiments of the coupled-enzyme assay were performed in the absence of PAPS, dopamine, MUS, SULT1A3, and K65ER68G of rat SULT1A1, respectively. Only the complete reaction renders the fluorometric activity of SULT1A3. K65ER68G of rat SULT1A1 is inactive toward DHEA, ADT, and dopamine in the conditions described above. Activity of SULT1A1 was determined according to the change of absorbency at 400 nm because of the elimination of free *p*-nitrophenol (ε = 10,500 $M^{-1}cm^{-1}$ at pH 7.0) as described previously (Yang et al., 1996). The reaction mixture consisted of 100 mM potassium phosphate buffer at pH 7.0, 1 to 100 nM (0.07–7 μg) SULT1A1, 50 μM PAPS, 5 mM 2-mercaptoethanol, and 5 μM *p*-nitrophenol at 37°C.

Substrate Binding. The dissociation constants (K_d) of PAP, DHEA, and ADT toward SULT2A1, respectively, were determined with a spectrofluorimeter as described previously (Zhang et al., 1998). The decrease in intrinsic fluorescence of protein at 340 nm was observed upon excitation at 280 nm when an aliquot amount of PAP was added into the mixture consisted of 100 mM potassium phosphate buffer at pH 7.0, 100 nM wild-type or mutant SULT2A1 and varying concentrations of PAP at 25°C with a final volume of 1.3 ml in a quartz cuvette of 1-cm square cross-section. In the formation of ternary dead-end complex, DHEA and ADT were added into the preincubated solution containing 0.5 μM wild type or mutants of SULT2A1, 100 mM potassium phosphate at pH 7.0, and 1 μM PAP at 25°C. Each data point was duplicated, and the difference was within 10%.

Analysis of Kinetic Data. Results of kinetic experiments were analyzed using nonlinear regression to fit the appropriate equation to the data. Kinetic data obtained from noninhibitory experiments were individually fit to the Michaelis-Menten equation, $v = V[S]/(K_m + [S])$, and substrate inhibition data were fitted to a substrate inhibition equation, $v = V[S]/\{K_m + [S](1 + [S]/K_i)\}$ (Cornish-Bowden, 1995). The rate constants (K_m, V_{max}, and K_i) were obtained using SigmaPlot 2001, version 7.0, and Enzyme Kinetics Module, version 1.1 (SPSS Inc., Chicago, IL). Data used represent mean values derived from two determinations.

Protein Crystallization and Data Collection. Crystallization of M137I and M137W mutants was performed by the hanging-drop vapor-diffusion method at 18°C. This condition was further refined to produce larger crystals using 2-μl hanging drops containing equal volumes of protein solution (1 μl) and a reservoir solution (1 μl) containing $(NH_4)_2SO_4$ (1.6 M), NaCl (100 mM), and HEPES (0.1 M) at pH 7.5. The crystals of M137I and M137W appeared within 3 days and grew to maximum dimensions after 7 days.

Crystallographic Data Collection and Processing. The crystals of diffraction quality were mounted on a Cryo-loop (0.1–0.2 mm), dipped briefly in 20% glycerol as a cryoprotectant solution, and

frozen in liquid nitrogen. X-ray diffraction data were collected at 110 K using the synchrotron radiation on the beamline BL13B1 at NSRRC (Hsinchu, Taiwan). The data were indexed and processed using the *HKL2000* program (Otwinowski and Minor, 1997). Details of the data statistics are given in Table 1.

Crystal Structure Determination and Refinement. The structures of the M137I and M137W were determined by molecular replacement as implemented in CNS v1.1 (Brunger et al., 1998) using the crystal structure of human dehydroepiandrosterone sulfotransferase (Protein Data Bank code 1OV4) (Chang et al., 2004) as a search model. The M137I and M137W molecule was located in the asymmetry unit after rotation and translation function searches. All refinement procedures were performed using CNS v1.1. The composite omitted electron $|2F_o - F_c|$ were calculated and visualized using O v11.0.4 (Jones et al., 1991), and the model was rebuilt and adjusted iteratively as required. Throughout the refinement, a random selection (10%) of the data were placed aside as a "free data set," and the model was refined against the rest of the data with $F > 0$ as a working set. The monomer protein model was initially refined by rigid-body refinement using the data from 30.0- to 3.0-Å resolution, for which the group temperature B values were first restrained to 20 Å^2. This refinement was followed by simulated annealing using a slow cooling protocol with a starting temperature 2500 K, provided in CNS, applied to all data between 20.0 and 2.6 and 3.0 Å for M137I and M137W, respectively. The bulk solvent correction was then applied, and group B factors were adjusted. After several cycles of positional and grouped B factor refinement interspersed with interactive modeling, the R-factors for the M137I and M137W complex decreased. The refinement then proceeded with another cycle of simulated annealing with a slow cooling with a starting temperature of 1000 K.

Model Validation. The correctness of stereochemistry of the model was verified using PROCHECK (Laskowski et al., 1993). The calculations of root-mean-square deviations (RMSDs) from ideality for bonds, angles, and dihedral and improper angles performed in CNS showed satisfactory stereochemistry. In a Ramachandran plot (Ramachandran and Sasisekharan, 1968), all of main chain dihedral angles were in the most favored and additionally allowed regions. The refinement statistics are given in Table 1.

Coordinates. Atomic coordinates for the crystal structures of M137I and M137W mutants described in this work have been deposited in the Protein Data Bank (access codes 2QP3 and 2QP4, respectively).

TABLE 1
Data collection and structure refinement statistics

	M137I/ADT	M137W/ADT
Crystal data collection	BL13B1/NSRRC	BL13B1/NSRRC
Wavelength (Å)	1.000	1.000
Temperature (K)	110	110
Space group	$P2_12_12$	$C222_1$
Unit-cell parameters (Å)		
a	76.28	109.41
b	131.72	133.02
c	44.55	76.30
Resolution range (Å)	30–2.59 (2.73–2.59)	30–3.0 (3.12–3.0)
No. of unique reflections	14,606	11,368
Completeness (%)	99.6 (99.3)	99.4 (97.7)
$I/\sigma_{(I)}$	42.5 (10.1)	19.5 (2.8)
Average redundancy	14.2	7.8
R_{sym} (I) (%)[a]	6.6 (30.6)	11.4 (70.0)
No. of proteins/A.U.	1	1
Refinement and statistics		
Resolution range (Å)	20–2.6	20–3.0
Number of reflections[b]	14,138	10,882
Number of total atoms	2269	2369
R_{work} (%)[c]	22.5	24.6
R_{free} (%)[d]	26.3	30.2
Average B-factors (Å^2)	46.46	72.11
R.M.S.D from ideal values		
Bond length (Å)	0.006	0.008
Bond angles (°)	1.22	1.39
Dihedral angles (°)	21.45	22.22
Improper torsion angles (°)	0.752	0.848

[a] $R_{sym} = \Sigma_h \Sigma_i [|I_i(h) - <I(h)>|/\Sigma_h \Sigma_i I_i(h)]$, where I_i is the ith measurement and $<I(h)>$ is the weighted mean of all measurements of I(h).
[b] Reflections of $2\sigma_I$ cutoff were applied in generating the refinement statistics.
[c] $R_{work} = \Sigma_h |F_o - F_c|/\Sigma_h F_o$, where F_o and F_c are the observed and calculated structure factor amplitudes of reflection h.
[d] R_{free} is as R_{work}, but calculated with 10% pf randomly chosen reflection omitted from the refinement.

Results

Predicting Critical Amino Acid Residues for Substrate Inhibition by the Comparison of the Structure of SULT2A1 Complexes. Comparison between the SULT2A1/DHEA and SULT2A1/PAP binary complex structures may reveal the alternative locations of the main regulatory amino acid residues when substrate is present or absent in the active site. The overall structure of the SULT2A1/PAP complex is very similar to that of the SULT2A1/DHEA complex, except for some residues and a loop from residues Tyr-231 to Gly-252 (Table 2). The RMSD value of this loop between the two structures is 6.67 Å for the backbone (excluding Lys-242 and Thr-243, which were not resolved in the SULT2A1/PAP binary complex structure). As shown in Fig. 1A, the main difference near the DHEA binding site between the two complexes is that the loop from residues Tyr-231 to Tyr-238 is closed in SULT2A1/PAP, whereas it is open in SULT2A1/DHEA (Pedersen et al., 2000; Rehse et al., 2002). Furthermore, in the SULT2A1/DHEA complex, several hydrophobic residues on this loop, including Tyr-231, Leu-234, and Tyr-238, are located near the DHEA molecule; these residues contribute to the hydrophobic nature of the

TABLE 2
RMSD values of SULT2A1/DHEA (1J99) and SULT2A1/PAP (1EFH) complex structures.
Superposition of these two known structures was created by Combinatorial Extension (CE) (Shindyalov and Bourne, 1998) and the root-mean-square deviation (RMSD) was calculated by Swiss-Pdb Viewer (Guex and Peitsch, 1997). The average RMSD of residues 4 to 230 and 253 to 279 was less than 2.5 Å.

Residues			RMSD		
Residue Nos.	1J99	1EFH	Backbone	Side Chain	All Atoms
				Å	
4–230			1.20	2.03	1.69
231	Tyr	Tyr	4.16	9.56	8.16
232	Ser	Ser	6.42	8.88	7.33
233	Leu	Leu	7.36	8.50	7.95
234	Leu	Leu	6.24	5.97	6.11
235	Ser	Ser	6.39	6.55	6.44
236	Val	Val	5.63	8.58	7.05
237	Asp	Asp	6.64	9.80	8.37
238	Tyr	Tyr	7.00	8.48	8.02
239	Val	Val	6.18	8.43	7.23
240	Val	Val	4.11	3.31	3.79
241	Asp	Asp	2.04	4.36	3.40
242	Lys	—[a]			
243	Thr	—[a]			
244	Gln	Gln	6.26	6.18	6.22
245	Leu	Leu	6.59	8.72	7.73
246	Leu	Leu	6.51	8.84	7.76
247	Arg	Arg	5.79	8.44	7.58
248	Lys	Lys	7.41	5.18	6.27
249	Gly	Gly	9.63	0	9.63
250	Val	Val	9.61	11.52	10.47
251	Ser	Ser	8.69	11.75	9.82
252	Gly	Gly	6.05	0	6.05
253–279			0.98	2.34	1.83
Average			2.13	2.86	2.54

[a] Structure in this region was not solved.

active site. In addition, in the SULT2A1/DHEA binary complex structure, Tyr-238 probably acts as the gate toward the substrate-binding cavity but moves away from the active site in the SULT2A1/PAP binary complex structure (Fig. 1A). It is therefore reasonable to speculate that Tyr-238 may play a critical role in regulating the release of substrate. As shown in Fig. 1B, the ADT molecule shares the same location as that of the DHEA molecule in the previously proposed alternative orientation (Rehse et al., 2002). The SULT2A1/DHEA and SULT2A1/ADT complex structures are quite similar at this region, including the loop described above, and the location of Tyr-238 residue.

Kinetic Analysis of Tyr-238 Mutants of SULT2A1. The hypothesized gate residue of Tyr-238 for regulating substrate inhibition, as revealed by the above structural comparison, was confirmed by site-directed mutagenesis. V_{max}, K_m, and K_i values of wild-type and Tyr-238 mutants (Y238A, Y238F, and Y238W of SULT2A1) were determined using DHEA or ADT as substrates (Table 3). Y238A of SULT2A1 exhibited no substrate inhibition when ADT was used as substrate and the K_i value of DHEA increased 7.4-fold compared with that of wild-type SULT2A1. The K_i values of DHEA and ADT for Y238F and Y238W of SULT2A1 also increased for approximately 2- to 3-fold compared with those of the wild type. The changes of K_m and V_{max} for Y238A, Y238F, and Y238W ranged only from approximately 0.3- to 1.3-fold whenever DHEA or ADT was used as substrate (Table 3). This observation, consistent with the above prediction base on structural analysis, showed that Tyr-238 was regulating the substrate inhibition and demonstrated that the size of this amino acid side chain was important.

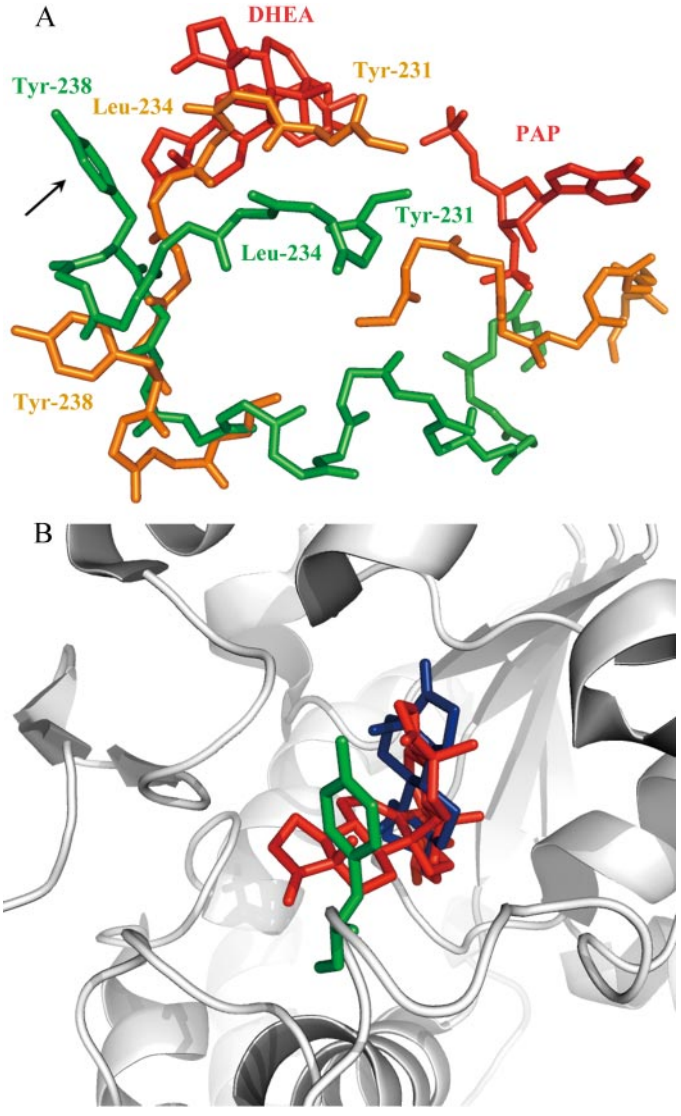

Fig. 1. Structures of the loop from residues Tyr-231 to Gly-252 of SULT2A1/PAP, SULT2A1/DHEA, and SULT2A1/ADT complexes. A, loop and substrate binding site. Superposition of this loop was performed between the SULT2A1/PAP (orange) and SULT2A1/DHEA (green) complex structures. The structure of SULT2A1/ADT at this region is very similar to that of SULT2A1/DHEA. The two ligands (DHEA and PAP) are colored in red, and the proposed entrance of substrate is marked by an arrow. B, SULT2A1/DHEA and the SULT2A1/ADT complex structures. Tyr-238 (green) was proposed to act as a gate residue for the substrate-binding site. The DHEA molecule was placed in two orientations and was colored in red; ADT molecule was colored in blue.

Predicting Amino Acid Residue Delineated the Orientations of DHEA and ADT in SULT2A1. Mutating Tyr-238 to alanine completely and partially eliminate the substrate inhibition for ADT and DHEA, respectively (Table 3), indicating that the additional amino acid(s) may be interacting with these two substrates in a different way because a single mutation (Tyr-238) is not capable of completely eliminating inhibition of both substrates. The complex structures of SULT2A1/DHEA and SULT2A1/ADT reveal two orientations for DHEA but only one for ADT, as described previously (Chang et al., 2004). Based on the available information, we might infer that the additional amino acid(s) that affect the substrate inhibition of DHEA might also affect its binding orientation in SULT2A1. To search for the possible amino acid(s), we superimposed the structures of SULT2A1/DHEA and SULT2A1/ADT on each other. Most of the amino acid residues hold the same positions in two complex structures, except for the side chains of Met-16, Ile-71, and Met-137 whose RMSD values (2.41, 2.50, and 2.40 Å, respectively) were noticeably higher than those of the others (Fig. 2). Both Met-16 and Ile-71 of the SULT2A1/DHEA and SULT2A1/ADT complex structures form similar van der Waals interactions toward ADT and DHEA in the two orientations. By contrast, the C_ε atom of the Met-137 residue in SULT2A1/ADT complex structure points inward to the substrate binding site, causes steric hindrance for ADT, and prevented it from forming additional orientation observed only for DHEA. The shortest distance would have been only 1.11 Å between C-12 of DHEA at this additional orientation and the C_ε atom of Met-137 in SULT2A1/ADT complex (Fig. 2). From the structural analysis between SULT2A1/DHEA and SULT2A1/ADT complexes, it is reasonable to propose that, in addition to Tyr-238, Met 137 may serve as the amino acid that modulates the substrate inhibition and binding orientations of DHEA and ADT.

Kinetic Analysis of Met-137 and Met-137/Tyr-238 Mutants of SULT2A1. The proposed effects of Met-137 on substrate inhibition were examined by mutational analysis of SULT2A1 at Met-137 and Tyr-238. When Met-137 of SULT2A1 was mutated to isoleucine (M137I) and valine (M137V), which contain smaller side chains, K_i values for ADT increase over 1 order of magnitude (28.6-fold for M137I and 11.1-fold for M137V) (Table 3). The K_i value increases only 5.4-fold when Met-137 was mutated to a larger side chain, tryptophan (M137W). Changes of K_i values for DHEA were in a similar

trend to those of ADT with smaller increases (5.9-, 8.7-, and 1.2-fold for M137I, M137V, and M137W, respectively) (Table 3). M137K was also prepared and exhibited no enzymatic activity, most probably because of the positive charge of lysine that interferes with the hydrophobicity of the binding site.

These observations were consistent with the above structural analysis that Met-137 side chain was a steric hindrance for ADT in SULT2A1/ADT complex but not for DHEA in SULT2A1/DHEA complex (Fig. 2). By removing this steric hindrance, additional binding orientation for ADT may form and result in considerable changes (over 1 order of magnitude) of their K_i values (M137I and M137V in Table 3). This proposal also agrees with our finding that the orientation of ADT may be disturbed when Met-137 is replaced with a smaller isoleucine (M137I/Y238A in Table 3) so that the substrate inhibition of ADT with M137I/Y238A can be observed. In contrast, by replacing a large side chain at Met-137 (M137W), additional steric hindrance may be created, and one of the binding orientations of DHEA may be removed. This also predicts that, with additional mutation on Y238A at Met-137, the substrate inhibition for DHEA may be completely eliminated. Double mutations on SULT2A1 at Met-137 and Tyr-238 confirm our hypothesis (M137W/Y238A in Table 3). Two other double mutants, M137V/Y238A and M137K/Y238A (Table 3), also exhibited expected properties. The K_i values obtained with M137V/Y238A were between those obtained with M137I/Y238A and M137W/Y238A. M137K/Y238A still exhibited no enzymatic activity similar to that of M137K.

Comparison of the Crystal Structure of Wild-Type, M137I, and M137W of SULT2A1. The data discussed above indicate that the additional substrate binding orientation modulated by Met-137 might be responsible for the substrate inhibition observed in Y238A only for DHEA but not for ADT (Table 3). The crystal structures of M137I and M137W in this study were determined and showed that the each global structure was similar to that of the wild type, either the SULT2A1/DHEA or SULT2A1/ADT complex structure. In Fig. 3, the structures of the residue Met-137 in SULT2A1 were compared with those of isoleucine (M137I) and tryptophan (M137W) in SULT2A1 mutants. Replacing Met-137 with tryptophan (M137W) obviously contributes to steric hindrance and prevents the formation of the additional orientation of DHEA. This structural information is consistent with our hypothesis that the additional orientation of DHEA is responsible for the substrate inhibition in Y238A. As shown in Table 3, the DHEA substrate inhibition in Y238A can be eliminated in M137W/Y238A. On the contrary, replacing Met-137 with isoleucine (M137I) may remove the steric hindrance and provides a space for the formation of additional orientation for ADT in SULT2A1 (Fig. 3). As shown in Table 3, the ADT substrate inhibition of Y238A can be regenerated with M137I/Y238A. Combination of the structural and kinetic data strongly supports our hypothesis that both Tyr-238 and Met-137 of SULT2A1 are responsible for the regulation of substrate inhibition as described above.

Dissociation Constants of PAP, DHEA, and ADT in Binary and Ternary Complex Structures of SULT2A1 and Its Mutants. It is important to show that this ternary complex is intact in SULT2A1 mutants (Y238A, M137I, M137W, M137I/Y238A and M137W/Y238A) to support our proposal that Met-137 and Tyr-238 directly modulate substrate inhibition. As shown in Table 4, the dissociation constants of PAP of SULT2A1/PAP binary complexes were the same among wild type and all the mutants. Tight binding of PAP (in the nanomolar range, as shown in Table 4) to the SULT2A1 and its mutants indicates that PAP binding site remains intact after such mutations. This information excludes the possibility that the change of K_i values reported in this study is due to the change of PAP binding to SULT2A1 mutants.

Affinity of either DHEA or ADT to SULT2A1/PAP binary complex was noticeably decreased whenever there is an Y238A mutant (Y238A, M137I/Y238A, and M137W/Y238A) compared with that with wild-type SULT2A1 (Table 4). Except for the DHEA with M137I, mutation at Met-137 (M137I or M137W) did not significantly affect the binding of either DHEA or ADT to the SULT2A1/PAP binary complex. The dissociation constants of ligands (PAP, DHEA, and ADT) and the double mutants of SULT2A1, M137I/Y238A and M137W/Y238A, are very similar to those with single mutant, Y238A (Table 4). These observations are consistent with the proposed function of Tyr-238 and Met-137 that the former acts to

TABLE 3

Rate constants of SULT2A1 wild type and mutants using DHEA and ADT as substrates

Sulfotransferase activity was measured as indicated under *Materials and Methods.*

SULT2A1	DHEA				ADT			
	K_m	V_{max}	V_{max}/K_m	K_i	K_m	V_{max}	V_{max}/K_m	K_i
	μM	*nmol/min/mg*		μM	μM	*nmol/min/mg*		μM
Wild type	2.5 ± 0.7	227 ± 42	91	6.1 ± 1.7	1.4 ± 0.8	203 ± 86	145	0.7 ± 0.4
Y238A	3.3 ± 0.3	191 ± 8.3	58	45 ± 4.9	1.4 ± 0.1	55 ± 1.3	39	N.A.
Y238F	1.1 ± 0.2	108 ± 8.2	98	12 ± 1.7	1.5 ± 0.6	134 ± 38	90	2.2 ± 0.9
Y238W	0.7 ± 0.1	71 ± 5.1	101	15 ± 2.9	0.7 ± 0.6	79 ± 44	113	1.2 ± 0.8
M137I	1.3 ± 0.2	68 ± 4.9	52	36 ± 6.8	0.2 ± 0.06	42 ± 5.1	208	20 ± 7.9
M137V	1.9 ± 0.6	70 ± 8.9	37	53 ± 19	0.7 ± 0.3	60 ± 12	86	7.8 ± 3.2
M137W	1.3 ± 0.6	112 ± 32	86	7.1 ± 3.7	0.6 ± 0.2	61 ± 14	52	3.8 ± 1.6
M137K	N.D.	N.D.	N.D.	N.D.	N.D.	N.D.	N.D.	N.D.
M137I/Y238A	3.6 ± 0.7	48 ± 3.9	13	170 ± 53	1.4 ± 0.3	30 ± 1.8	22	159 ± 38
M137V/Y238A	6.5 ± 1.1	62 ± 4.0	9.5	466 ± 140	3.6 ± 0.4	37 ± 0.9	10	N.A.
M137W/Y238A	4.2 ± 0.3	97 ± 1.8	23	N.A.	2.0 ± 0.3	63 ± 2.2	31	N.A.
M137K/Y238A	N.D.	N.D.	N.D.	N.D.	N.D.	N.D.	N.D.	N.D.
V260E[a]	1.6 ± 0.4	160 ± 26	100	7.1 ± 1.9	1.4 ± 0.8	176 ± 74	126	1.2 ± 0.7
Y238A/V260E[a]	2.2 ± 0.1	144 ± 4.3	66	55 ± 4.8	1.8 ± 0.2	48 ± 1.4	27	N.A.

N.A., not applicable (substrate inhibition was not observed); N.D., not determined due to undetectable or low levels of activity.

[a] Monomer mutant of SULT2A1.

prevent the release of bound substrate, whereas the latter modulates the orientations of bound substrate in the substrate inhibition mode.

Substrate Inhibition in SULT2A1 Monomer. To examine the previous hypothesis that dimerization results in substrate blocking, the monomer mutant (V260E) of SULT2A1, designated in the KTVE motif (Petrotchenko et al., 2001), along with a double mutant, Y238A/V260E (Table 3), were constructed to comprehend the substrate inhibition of SULT2A1. The wild-type SULT2A1 (homodimer) was found to have kinetic constants similar to those of the mutant monomer. Furthermore, the pattern of substrate inhibition in monomer mutant (V260E in Table 3) is the same as that of wild-type SULT2A1. The mutation of monomer mutant at Tyr-238 (Y238A/V260E in Table 3) also gives exactly the same substrate inhibition pattern as that of Y238A of SULT2A1 (Table 3). Data obtained from this study indicates that dimer or monomer of SULT2A1 does not play an important role for the exhibition of substrate inhibition.

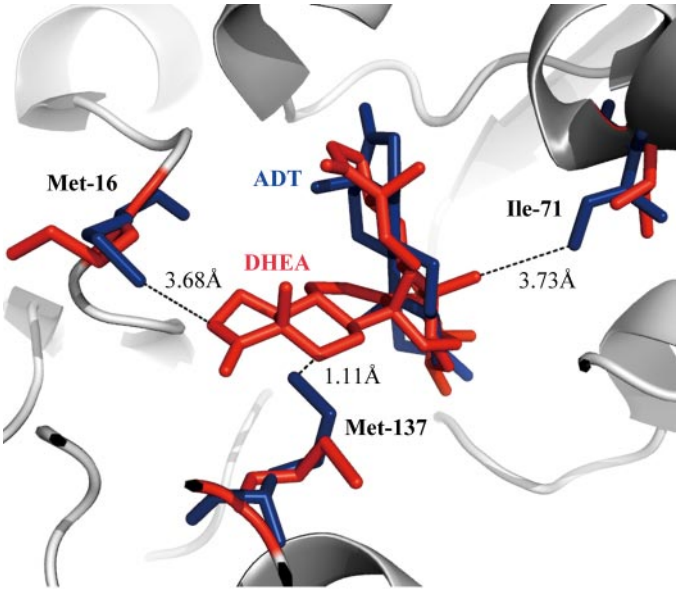

Fig. 2. Binding modes of DHEA and ADT molecules in SULT2A1. Comparison of the binding modes was performed between the SULT2A1/DHEA (red) and the SULT2A1/ADT (blue) complex structures. The residues Met-16, Ile-71, and Met-137 around the DHEA and ADT molecules are shown. DHEA showed van der Waals interactions (shown by dotted lines) with Met-16, Ile-71, and Met-137 with C-16, C-19, and C-12 of DHEA, respectively.

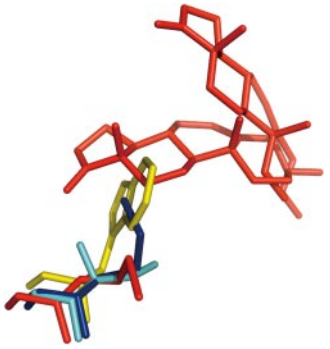

Fig. 3. Superimposition of the solved structures of wild-type, M137I, and M137W SULT2A1. The crystal structures of M137I (cyan) and M137W (yellow) are superimposed to the previous solved structures, SULT2A1/DHEA (red) and SULT2A1/ADT (blue), at Met-137. The DHEA in SULT2A1 complex structure is also shown and colored in red.

Functional Analysis of Tyr-238 and Met-137 Corresponding Residues in Other Sulfotransferases. The multiple sequence and structure alignments of some solved-structure sulfotransferases are shown in Fig. 4. In the upper left of Fig. 4, the residues corresponding to Tyr-238 of SULT2A1 have been highlighted and are as follows: Phe-247 of human SULT1A1, Leu-247 of human SULT1A3, Met-247 of mouse SULT1E1, and Leu-249 of human SULT2B1_v1 (Kakuta et al., 1997; Gamage et al., 2003; Lee et al., 2003; Lu et al., 2005). This comparison leads us to hypothesize that the Tyr-238 corresponding residue in other sulfotransferases may play a similar role in substrate inhibition because these residues all demonstrate possible steric hindrance for the release of substrate from the substrate-binding cavity, and therefore they may modulate substrate inhibition for their own preferred substrates. To characterize the function of the SULT2A1 Tyr-238 corresponding residues in other sulfotransferases, further mutational analysis was conducted with SULT1A1 and SULT1A3 at Phe-247 and Leu-247 residue, respectively (Table 5). Compared with those of wild-type SULT1A1, the K_i value of F247A (with *p*-nitrophenol as substrate) increased approximately 12-fold, the V_{max}/K_m value increased approximately 3-fold, and K_m remained pretty much the same. The K_i value of dopamine for SULT1A3 is much higher than that of *p*NP for SULT1A1 (Table 5). The positively charged dopamine at the assay condition may contribute to this difference. Mutations at Leu-247 of SULT1A3 give K_i values comparable with the size of the side chain of the mutated amino acid (the larger the amino acid side chain, the lower the K_i value) as shown in Table 5 for L247A and L247Y. The data from these investigations support our hypotheses that substrate inhibition in SULT2A1 is modulated by Tyr-238, and that analogous residues of Tyr-238 in other cytosolic sulfotransferases play similar roles with respect to substrate inhibition.

Discussion

The study in structure and function of enzymes has been greatly facilitated as a result of an expansion by means of their X-ray crystal structures. Crystal structures of SULT2A1 containing ADT (Chang et al., 2004), DHEA (Rehse et al., 2002), and PAP (Pedersen et al., 2000) have been reported. DHEA has been found to have two binding orientations in SULT2A1 (Rehse et al., 2002); however, bound ADT possesses only one, in

TABLE 4

Dissociation constants of PAP, DHEA, and ADT in wild-type and mutated SULT2A1

Dissociation constants were determined with spectrofluorimeter as indicated under *Materials and Methods.* The dissociation constants of binary complex were determined with PAP (5–365 nM) and SULT2A1 (100 nM). The dissociation constants of ternary complex were determined with DHEA (0.1–50 μM) or ADT (0.1–50 μM) and SULT2A1 (0.5 μM) in the presence of PAP (1 μM).

SULT2A1	Binary Complex PAP	Ternary Complex	
		DHEA	ADT
	nM	*μM*	
Wild type	40.7 ± 8.2	0.8 ± 0.05	0.4 ± 0.04
Y238A	48.7 ± 8.6	6.9 ± 0.3	3.2 ± 0.1
M137I	44.2 ± 8.4	1.9 ± 0.3	0.4 ± 0.06
M137W	49.2 ± 7.8	0.6 ± 0.07	0.3 ± 0.03
M137I/Y238A	32.2 ± 7.3	7.2 ± 0.4	2.4 ± 0.4
M137W/Y238A	49.4 ± 8.1	3.7 ± 0.6	2.3 ± 0.4

which it is flipped over along the long axis of the DHEA relative to the proposed alternative orientation (Chang et al., 2004). The previously proposed alternative orientation of DHEA was speculated to be a substrate-inhibition orientation, owing to the fact that it placed O-3 hydroxyl group of DHEA with respect to His-99 for 2.9 Å away, and closer to the modeled PAP. Furthermore, it contained more van der Waals interactions with hydrophobic residues than the proposed catalytic orientation (Rehse et al., 2002). Prior study (Gamage et al., 2005) however, suggested that this would not result in substrate inhibition, because this would require a relative increase in the proportion of the proposed alternative orientation, whereas the substrate concentration increases. It might imply that both the orientations of DHEA could cause substrate inhibition while PAP remained in the active site to form ternary dead-end complex. In this report, we identified two amino acids (Met-137 and Tyr-238) responsible for modulating substrate inhibition of DHEA and ADT and were able to provide experimental evidences to show that both substrate binding orientations indeed cause substrate inhibition.

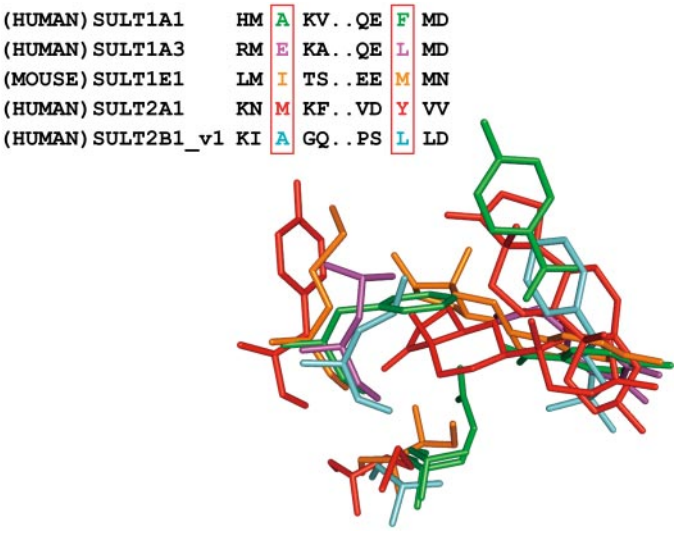

Fig. 4. Multiple sequence and structure alignment of Tyr-238 and Met-137 corresponding residues among some solved-structure cytosolic sulfotransferases. The in-position residues of Tyr-238 (top left) of SULT2A1 complex (red) are Phe-247 of human SULT1A1 (green), Leu-247 of human SULT1A3 (magenta), Met-247 of mouse SULT1E1 (orange), Leu-249 of human SULT2B1_v1 (cyan). The in-position residues of Met-137 (bottom center) of SULT2A1 complex are Ala-146 of human SULT1A1, Glu-146 of human SULT1A3, Ile-146 of mouse SULT1E1, and Ala-148 of human SULT2B1_v1. The substrates (two orientations on the right) of sulfotransferases are DHEA, *p*NP, dopamine, 17β-estradiol, and 2-[*N*-cyclohexylamino]ethane sulfonic acid for SULT2A1, SULT1A1, SULT1A3, SULT1E1, and SULT2B1_v1, respectively. Superposition of these known-structure sulfotransferases was created by combinatorial extension (CE) (Shindyalov and Bourne, 1998), and the multiple sequence alignment was produced by ClustalW (Thompson et al., 1994).

The bound orientations observed for DHEA and ADT might be in the substrate inhibition mode because the crystals were usually formed under high concentration of ligands, although PAP was not present in the solved crystal structures of SULT2A1/DHEA and SULT2A1/ADT (Rehse et al., 2002; Chang et al., 2004). Dissociation constants of DHEA for SULT2A1 and its mutants at Tyr-238 and Met-137 (Table 4) also indicate that substrate inhibition may be induced by two possible binding orientations for DHEA because the substrate inhibition could be eliminated only after two specific mutations (M137W/Y238A in Table 3). According to the crystal structures of SULT2A1 (Fig. 1B), Tyr-238 has weak interactions with ADT, and the closest distance between Tyr-238 and the substrates is approximately 4.6 Å. Structural analyses among SULT2A1 complexes (Fig. 1, A and B) strongly suggest that Tyr-238 acts as a gate residue to regulate the release of substrate from the substrate-binding cavity in a ternary dead-end complex. The dissociation constants of ternary dead-end complex shown in Table 4 also support this implication. K_d values of both DHEA and ADT increased significantly when Tyr-238 was mutated to alanine. However, mutation of Tyr-238 alone could not completely eliminate DHEA substrate inhibition (Y238A in Table 3), indicating the existence of an additional substrate inhibition mode for DHEA but not for ADT. Structural analysis showed that Met-137 is closely interacting with DHEA and ADT and may modulate the substrate binding orientation (Fig. 2). This scheme agrees with the experimental data that further mutation on Y238A at Met-137 not only can completely eliminate substrate inhibition for DHEA (M137W/Y238A in Table 3) but can also create substrate inhibition for ADT (M137I/Y238A in Table 3). These data strongly suggest that DHEA exists in only one orientation in M137W/Y238A and ADT presents in two orientations in M137I/Y238A. Comparison of the solved crystal structures shown in Fig. 3 gives additional support for the proposed substrate binding orientations in these mutants.

As shown in Fig. 4, other cytosolic sulfotransferases may also provide space for substrates with two binding orientations. It has been proposed that substrate inhibition in SULT1A1 by estradiol could occur from the misorientation of substrate in the complex (Gamage et al., 2005). The presence of two *p*NP molecules in the crystal structure of SULT1A1 was postulated to explain cooperativity at low and inhibition at high substrate concentrations, respectively (Barnett et al., 2004). For SULT2A1, the K_i values shown in Table 3 indicate that Met-137 and Tyr-238 may modulate substrate inhibition at low and high K_i values, respectively. For ADT, the K_i value is significantly increased when the additional substrate binding orientation is proposed to present in the enzyme (M137I

TABLE 5

Rate constants of SULT1A1, SULT1A3 and their mutants

Sulfotransferase activity was measured as indicated under *Materials and Methods*.

Enzyme	Substrate	K_m	V_{max}	V_{max}/K_m	K_i
		μM	*nmol/min/mg*		μM
SULT1A1					
Wild type	*p*-Nitrophenol	2.2 ± 1.0	323 ± 116	147	0.8 ± 0.4
F247A		3.2 ± 0.8	1437 ± 217	449	9.4 ± 2.1
SULT1A3					
Wild type	Dopamine	6.8 ± 0.9	623 ± 30	92	174 ± 23
L247A		22 ± 1.2	1149 ± 32	52	282 ± 22
L247Y		36 ± 14	1669 ± 457	46	61 ± 26

and M137I/Y238A in Table 3). The binding of substrates to Y238A is significantly loosened with PAP and enzyme complex (Table 4). This may either totally eliminate substrate inhibition (for ADT) or significantly decrease the substrate inhibition contribution from the substrate bound at the additional orientation (for DHEA). This scheme is consistent with the K_i value described previously for the reduced form of rat SULT1A1 that K_i is proposed to be determined by the binding constant of substrate and PAP/enzyme binary complex (Marshall et al., 2000).

Other possible causes for substrate inhibition proposed previously (Petrotchenko et al., 2001) were also examined in this study. In a previous study on SULT2A1/PAP complex structure (Pedersen et al., 2000), the loop of residues 231 to 252 shown in Fig. 1A was speculated to prevent substrate binding while being involved in the dimer interface. This implies that the dimer may be an inactive form, with the second subunit of the dimer contributing to the locking in the substrate-blocking loop. Dimerization of SULT2A1 is not important for the substrate inhibition, because exactly the same substrate inhibition patterns were observed for enzyme monomer, dimer and their mutants (Table 3).

The cause of sulfotransferase substrate inhibition has been attributed to the formation of an enzyme, substrate, and PAP ternary complex (Duffel and Jakoby, 1981; Zhang et al., 1998). The binding of PAP is critical for the formation of the ternary complex (Hsiao and Yang, 2002), and affinity of PAP has been shown to have profound effects on the activity of sulfotransferases (Yang et al., 1996; Marshall et al., 2000). Binding of PAP may significantly affect the substrate binding (Hsiao and Yang, 2002) and in turn affect substrate inhibition. This indicates that the changes of PAP affinity to sulfotransferase can affect substrate inhibition and enzyme activity. For example, rat SULT1A1 has been shown to significantly alter the transfer and physiological reactions in various redox states (Marshall et al., 1997). Mutation at other amino acid may also alter the PAP affinity to sulfotransferase (Yang et al., 1996; Hsiao and Yang, 2002). Mutation at Met-137 and Tyr-238 did not affect the nucleotide binding affinity to SULT2A1 (Table 4). In addition, the variations of the dissociation constants of DHEA and ADT in Tyr-238 and Met-137 mutants (Table 4) is consistent with what would be expected for the proposed functions of these two amino acids. Tyr-238 is proposed to modulate the release of bound substrate and can significantly affect the dissociation constants of substrates when mutated.

In contrast, Met-137 is proposed to modulate the binding orientation of substrates and may not significantly change the dissociation constants of substrates when mutated. Comparison of Met-137 and its corresponding residues in other sulfotransferases is shown in lower middle of Fig. 4. It is very interesting to observe that substrates used for various cytosolic sulfotransferase, shown on the upper right side of Fig. 4, all align in either direction like those of DHEA in human SULT2A1 (Figs. 2 and 4). Human SULT1A1 contains two smaller substrates (*p*NP) that also locate in the two directions, respectively. Although Met-137 is postulated to function as modulator of substrate orientation in SULT2A1, it may not have the same function in other sulfotransferases. In fact, a nearby Val-148, instead of corresponding Ala-146 of human SULT1A1, interacts directly with *p*NP (Barnett et al., 2004). However, this comparison indicates that the two orientations of substrate binding in cytosolic sulfotransferases may be a common feature, and it should be interesting to explore its functional meaning in enzyme catalysis.

The overall proposed model for the substrate binding orientation and inhibition modulated by Met-137 and Tyr-238 of SULT2A1 is depicted in Fig. 5. Wild-type SULT2A1 exhibited substrate inhibition by using either DHEA or ADT as substrates while the PAP was present. In the mutant Y238A, no substrate inhibition could be observed for ADT (with only one binding orientation) and less significant substrate inhibition for DHEA (with two binding orientations) than that of wild-type SULT2A1. Mutation at Met-137 proposed to regulate the substrate binding orientation in this study could not completely eliminate substrate inhibition (M137I and M137W in Table 3) either the mutant contained space for two substrate binding orientations (M137I) or for only one sub-

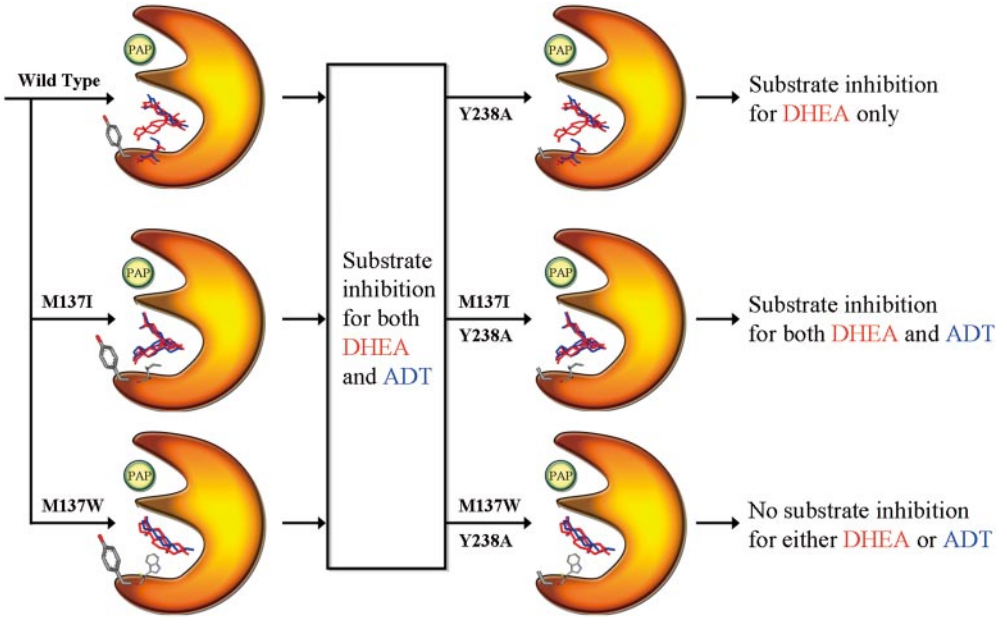

Fig. 5. Schematic illustration of SULT2A1 substrate binding orientation and inhibition was modulated by Met-137 and Tyr-238. The ternary dead-end complex was conceived of presence with PAP, DHEA, or ADT simultaneously. DHEA (red) and ADT (blue) compound structures are shown in one or two possible substrate binding orientations in SULT2A1 and its mutants. Tyr-238 is depicted as a gate residue modulating the release of bound substrate. Met-137 (red in SULT2A1/DHEA and blue in SULT2A1/ADT complex structures) is depicted as a stereo hindrance residue modulating the substrate binding orientation.

strate binding orientation (M137W). The relationship between the substrate binding orientations and substrate inhibition was uncovered when double mutations at Tyr-238 and Met-137 were examined. Although K_i values of both ADT and DHEA in mutant M137I/Y238A increase significantly compared with those of M137I and wild-type SULT2A1 (Table 3), substrate inhibition could not be completely removed because this mutant contains space for two binding orientations for both substrates. In contrast, M137W/Y238A exhibited no substrate inhibition by using either DHEA or ADT as substrate because this mutant can accommodate substrates in only one binding orientation.

Finally, the corresponding residues of SULT2A1 Tyr-238 in other cytosolic sulfotransferases were found to exhibit similar function in modulating substrate inhibition. Our study confirmed that Phe-247 of SULT1A1, which corresponds to Tyr-238 of SULT2A1, was also important for substrate inhibition of *p*NP (Table 5). Previous research on substrate inhibition of SULT1A1 (Gamage et al., 2003; Barnett et al., 2004) revealed that SULT1A1 could accommodate two *p*NP, which led to the substrate inhibition. Likewise, a higher or lower K_i value of dopamine was obtained for SULT1A3 when Leu-247, the corresponding residue to SULT2A1 Tyr-238, was mutated to a smaller or larger amino acid, alanine or tyrosine, respectively (Table 5). It is also consistent with the above discussion that the substrate inhibition (*p*NP) of SULT1A1 could not be completely eliminated (Table 5) with a single mutation at the corresponding position of Tyr-238 of SULT2A1 (i.e., Phe-247), because two possible binding orientations (and two bound substrates) also exist for *p*NP in SULT2A1 (Fig. 4). We therefore propose that the Tyr-238 and its corresponding residues in other cytosolic sulfotransferases play the similar role on regulating the release of substrate.

In conclusion, we propose that the substrate inhibition in SULT2A1 could occur from either orientation of substrate binding in the complex. The proposed function of Tyr-238 and Met-137 in SULT2A1 in this study might also be a model to explain how the substrate inhibition is modulated in other cytosolic sulfotransferases.

Acknowledgments

We thank Quillan Huang for proofreading the manuscript.

References

Barnett AC, Tsvetanov S, Gamage N, Martin JL, Duggleby RG, and McManus ME (2004) Active site mutations and substrate inhibition in human sulfotransferase 1A1 and 1A3. *J Biol Chem* **279:**18799–18805.

Brunger AT, Adams PD, Clore GM, DeLano WL, Gros P, Grosse-Kunstleve RW, Jiang JS, Kuszewski J, Nilges M, Pannu NS, et al. (1998) Crystallography & NMR system: a new software suite for macromolecular structure determination. *Acta Crystallogr D* **54:**905–921.

Chang HJ, Shi R, Rehse P, and Lin SX (2004) Identifying androsterone (ADT) as a cognate substrate for human dehydroepiandrosterone sulfotransferase (DHEA-ST) important for steroid homeostasis: structure of the enzyme-ADT complex. *J Biol Chem* **279:**2689–2696.

Chen G, Banoglu E, and Duffel MW (1996) Influence of substrate structure on the catalytic efficiency of hydroxysteroid sulfotransferase STa in the sulfation of alcohols. *Chem Res Toxicol* **9:**67–74.

Chen WT, Liu MC, and Yang YS (2005) Fluorometric assay for alcohol sulfotransferase. *Anal Biochem* **339:**54–60.

Cornish-Bowden A (1995) *Analysis of Enzyme Kinetic Data*, pp 118–122, Oxford University Press, Oxford, UK.

Duffel MW and Jakoby WB (1981) On the mechanism of aryl sulfotransferase. *J Biol Chem* **256:**11123–11127.

Falany C and Roth JA (1993) Properties of human cytosolic sulfotransferases involved in drug metabolism, in *Human Drug Metabolism: from Molecular Biology to Man* (Jeffery EH ed) pp 101–115, CRC Press, Inc. Boca Raton, FL.

Falany CN (1997) Enzymology of human cytosolic sulfotransferases. *FASEB J* **11:** 206–216.

Gamage NU, Duggleby RG, Barnett AC, Tresillian M, Latham CF, Liyou NE, McManus ME, and Martin JL (2003) Structure of a human carcinogen-converting enzyme, SULT1A1. Structural and kinetic implications of substrate inhibition. *J Biol Chem* **278:**7655–7662.

Gamage NU, Tsvetanov S, Duggleby RG, McManus ME, and Martin JL (2005) The structure of human SULT1A1 crystallized with estradiol. An insight into active site plasticity and substrate inhibition with multi-ring substrates. *J Biol Chem* **280:**41482–41486.

Ganguly TC, Krasnykh V, and Falany CN (1995) Bacterial expression and kinetic characterization of the human monoamine-sulfating form of phenol sulfotransferase. *Drug Metab Dispos* **23:**945–950.

Glatt H (1997) Sulfation and sulfotransferases 4: bioactivation of mutagens via sulfation. *FASEB J* **11:**314–321.

Guex N and Peitsch MC (1997) SWISS-MODEL and the Swiss-PdbViewer: an environment for comparative protein modeling. *Electrophoresis* **18:**2714–2723.

Hsiao YS and Yang YS (2002) A single mutation converts the nucleotide specificity of phenol sulfotransferase from PAP to AMP. *Biochemistry* **41:**12959–12966.

Jones TA, Zou JY, Cowan SW, and Kjeldgaard M (1991) Improved methods for building protein models in electron density maps and the location of errors in these models. *Acta Crystallogr A* **47:**110–119.

Kakuta Y, Pedersen LG, Carter CW, Negishi M, and Pedersen LC (1997) Crystal structure of estrogen sulphotransferase. *Nat Struct Biol* **4:**904–908.

Kakuta Y, Pedersen LC, Chae K, Song WC, Leblanc D, London R, Carter CW, and Negishi M (1998) Mouse steroid sulfotransferases: substrate specificity and preliminary X-ray crystallographic analysis. *Biochem Pharmacol* **55:**313–317.

Laemmli UK (1970) Cleavage of structural proteins during the assembly of the head of bacteriophage T4. *Nature* **227:**680–685.

Laskowski RA, MacArthur MW, Moss DS, and Thornton JM (1993) PROCHECK: A program to check the stereochemical quality of protein structures. *J Appl Cryst* **26:**283–291.

Lee KA, Fuda H, Lee YC, Negishi M, Strott CA, and Pedersen LC (2003) Crystal structure of human cholesterol sulfotransferase (SULT2B1b) in the presence of pregnenolone and 3′-phosphoadenosine 5′-phosphate. Rationale for specificity differences between prototypical SULT2A1 and the SULT2BG1 isoforms. *J Biol Chem* **278:**44593–44599.

Lu JH, Li HT, Liu MC, Zhang JP, Li M, An XM, and Chang WR (2005) Crystal structure of human sulfotransferase SULT1A3 in complex with dopamine and 3′-phosphoadenosine 5′-phosphate. *Biochem Biophys Res Commun* **335:**417–423.

Marcus CJ, Sekura RD, and Jakoby WB (1980) A hydroxysteroid sulfotransferase from rat liver. *Anal Biochem* **107:**296–304.

Marshall AD, Darbyshire JF, Hunter AP, McPhie P, and Jakoby WB (1997) Control of activity through oxidative modification at the conserved residue Cys66 of aryl sulfotransferase IV. *J Biol Chem* **272:**9153–9160.

Marshall AD, McPhie P, and Jakoby WB (2000) Redox control of aryl sulfotransferase specificity. *Arch Biochem Biophys* **382:**95–104.

Mulder GJ and Jakoby WB (1990) Sulfation in conjugation reactions, in *Drug Metabolism* (Mulder GJ and Jakoby WB eds) pp 107–161, Taylor and Francis, Ltd., London.

Otwinowski Z and Minor W (1997) Processing of X-ray diffraction data collected in oscillation mode. *Methods Enzymol* **276:**307–326.

Pedersen LC, Petrotchenko EV, and Negishi M (2000) Crystal structure of SULT2A3, human hydroxysteroid sulfotransferase. *FEBS Lett* **475:**61–64.

Petrotchenko EV, Pedersen LC, Borchers CH, Tomer KB, and Negishi M (2001) The dimerization motif of cytosolic sulfotransferases. *FEBS Lett* **490:**39–43.

Raftogianis RB, Wood TC, and Weinshilboum RM (1999) Human phenol sulfotransferases SULT1A2 and SULT1A1: genetic polymorphisms, allozyme properties, and human liver genotype-phenotype correlations. *Biochem Pharmacol* **58:**605–616.

Ramachandran GN and Sasisekharan V (1968) Conformation of polypeptides and proteins. *Adv Protein Chem* **23:**283–438.

Rehse PH, Zhou M, and Lin SX (2002) Crystal structure of human dehydroepiandrosterone sulphotransferase in complex with substrate [published erratum appears in *Biochem J* **364:**888, 2002]. *Biochem J* **364:**165–171.

Sakakibara Y, Takami Y, Nakayama T, Suiko M, and Liu MC (1998) Localization and functional analysis of the substrate specificity/catalytic domains of human M-form and P-form phenol sulfotransferases. *J Biol Chem* **273:**6242–6247.

Shindyalov IN and Bourne PE (1998) Protein structure alignment by incremental combinatorial extension (CE) of the optimal path. *Protein Eng* **11:**739–747.

Sugiyama Y, Stolz A, Sugimoto M, Kuhlenkamp J, Yamada T, and Kaplowitz N (1984) Identification and partial purification of a unique phenolic steroid sulphotransferase in rat liver cytosol. *Biochem J* **224:**947–953.

Thompson JD, Higgins DG, and Gibson TJ (1994) CLUSTAL W: improving the sensitivity of progressive multiple sequence alignment through sequence weighting, position-specific gap penalties and weight matrix choice. *Nucleic Acids Res* **22:**4673–4680.

Varin L and Ibrahim RK (1992) Novel flavonol 3-sulfotransferase. Purification, kinetic properties, and partial amino acid sequence. *J Biol Chem* **267:**1858–1863.

Weinshilboum R and Otterness D (1994) Sulfotransferase enzyme in conjugation-deconjugation reactions, in *Drug Metabolism and Toxicity* (Kaufmann FC ed) pp 45–78, Springer-Verlag, Berlin.

Yang YS, Marshall AD, McPhie P, Guo WX, Xie X, Chen X, and Jakoby WB (1996) Two phenol sulfotransferase species from one cDNA: nature of the differences. *Protein Expr Purif* **8:**423–429.

Zhang H, Varlamova O, Vargas FM, Falany CN, and Leyh TS (1998) Sulfuryl transfer: the catalytic mechanism of human estrogen sulfotransferase. *J Biol Chem* **273:**10888–10892.

Address correspondence to: Dr. Yuh-Shyong Yang, Department of Biological Science and Technology, National Chiao Tung University, Hsinchu, Taiwan, ROC, 75 Po-Ai Street, Hsinchu30050, Taiwan, ROC. E-mail: ysyang@faculty.nctu.edu.tw